JOURNAL OF ELECTROMAGNETIC ENGINEERING AND SCIENCE, VOL. 24, NO. 6, 674~676, NOV. 2024

https://doi.org/10.26866/jees.2024.6.l.24
ISSN 2671-7263 (Online) · ISSN 2671-7255 (Print)

Two-Step Adaptive Target Detection Scheme Using Beam-Steering FMCW Radar Sensors

Bong-seok Kim[a] · Young-seok Jin[b] · Jieun Bae[c] · Eugin Hyun[*,d]

Abstract

This letter proposes a two-stage adaptive target detection approach using a beam-steered frequency-modulated continuous wave (FMCW) radar sensor. In the first step, coarse estimation was performed using multiple sharped beams, where the presence of a target was determined using only a portion of the sampled beat signals. In the second step, a high-resolution range-Doppler (RD) map was generated using the entire information about the beat signal pertaining to the transmitted beams estimated to contain the target. Angle estimation was accomplished through digital beamforming based on the enhanced RD map. Furthermore, to verify the effectiveness of the proposed algorithm, high-resolution target detection experiments were conducted using a 24-GHz FMCW radar, while complexity reduction was evaluated in terms of the required memory size.

Key Words: Beam Steering, FMCW Radar, Low Complexity, Phased Array, Range-Doppler Map.

I. Introduction

Radar sensors have emerged as promising components for use in technological applications related to various domains, including automotive, surveillance, aerospace, and defense [1–4]. One of their remarkable advantages is their ability to operate in a variety of weather conditions, since the electromagnetic waves in radar sensors are not affected by fog, rain, or snow. In this context, the emergence of beam steering-based phased array (PA) systems has brought about a paradigm shift in the field of radar technology by revolutionizing the functionality and performance of radar sensors [5, 6]. Compared to mechanical beam steering, PA-based beam steering has significant merits—reduced size and weight of antennas, fast speed, high efficiency, and low power consumption. Moreover, it enables improved target detection performance, as it involves radiating a beam sharpened by beam steering to focus on a target. Notably, in a previous work [6], clutter suppression was observed when a radar module designed using a radar chipset was employed. However, as beams become sharper, a greater number of them need to be radiated. This has increased the amount of signal processing that must be performed at the receiving end, which in turn increases the complexity.

To address this issue, this letter proposes an algorithm featuring a two-step process. First, the proposed algorithm uses only a portion of the sampled beat signals to determine whether a target exists. Subsequently, it generates a high-resolution range-Doppler (RD) map by accounting for all sampled beat signals for the beams estimated to contain a target. The angle position of target is then estimated by performing digital beamforming (DBF) based on the improved RD map. Furthermore, to verify the effectiveness of the proposed algorithm, we generated the RD map using a 24-GHz frequency modulate continuous wave (FMCW) radar along with two stationary targets—one equipped with a Doppler generator—located at different distances and angles. The experimental results showed that the proposed algorithm successfully generated high-resolution RD maps, despite reduced overall complexity. Additionally, the effectiveness of the reduction in complexity was analyzed by comparing the required memory sizes.

II. System Model

An FMCW radar system equipped with P transmitting (TX) and

Manuscript received January 16, 2024 ; Accepted March 13, 2024. (ID No. 20240116-013J)
Department of Future Automotive Technology, Daegu Gyeongbuk Institute of Science and Technology, Daegu, Korea.
[a]https://orcid.org/0000-0003-4949-0381 [b]https://orcid.org/0000-0003-3473-4734
[c]https://orcid.org/0009-0002-9921-2275 [d]https://orcid.org/0000-0001-8196-7173
[*]Corresponding Author: Eugin Hyun (e-mail: braham@dgist.ac.kr)

Q receiving (RX) phased array antennas was employed, with K TX beams transmitted within the time of one frame T_f, as shown in Fig. 1(a) and 1(b). The angle of the k-th TX beam is denoted by $\theta_k^{\mathrm{TX}}(=-\theta_{\max}+(k-1)\theta_\Delta)$, where $\theta_{\max}$ is the maximum angle of the TX beam and θ_Δ is the interval between adjacent TX beam angles, meaning that $\theta_k^{\mathrm{TX}}=[-40°,-30°,\dots,40°]$ when $\theta_{\max}=40°$ and $\theta_\Delta=10°$. As shown in Fig. 1(b), when a TX FMCW signal with time duration T and bandwidth B is transmitted, it is received by the RX antenna after a time delay of the m-th target τ_m. The RX signal was mixed with the TX signal to obtain the analog digital convert (ADC) beat signal of N_s samples. Therefore, the beat signal at the k-th beam, q-th RX antenna, and l-th frame can be denoted by $y_k^{(q,l)}[n]$, expressed as follows:

$$y_k^{(q,l)}[n]=\sum_{m=1}^{M} a_{m,k}^{(q,l)}\eta_m^{n-1}v_m^{l-1}\psi_{m,k}^{q-1}+w_k^{(q,l)}[n]. \quad (1)$$

Here, M refers to the number of targets, $a_{m,k}^{(q,l)}$ signifies the complex amplitude corresponding to the m-th target, and $w_k^{(q,l)}[n]$ is the additive Gaussian white noise term. In addition, η_m, v_m, and $\psi_{m,k}$ are sinusoid signals representing the range, velocity, and direction-of-arrival (DOA), respectively. They can be expressed as follows: $\eta_m=\exp(-j2\pi\mu\tau_m t_s)$, where μ is the slope and t_s is the sampling time interval; $v_m=\exp(j2\pi f_{D,m}T_f)$, where $f_{D,m}$ is the Doppler frequency; and $\psi_{m,k}=\exp(jq\pi\sin(\theta_{m,k}))$, with $\theta_{m,k}$ being the DOA term.

III. Proposed Two-Step Adaptive Target Detection Method

The structure of the proposed two-step algorithm is illustrated in Fig. 2. In the first step, only a portion of the beat signals is used to coarsely estimate the region of the target. In Fig. 2, $N_s^{(\mathrm{r})}$ and $L^{(\mathrm{r})}$ indicate the reduced number of samples of N and L, respectively—for example, $N_s^{(\mathrm{r})}=N_s/4$ or $L^{(\mathrm{r})}=L/2$. This serves to reduce unnecessary computational complexity. Next, to enhance the signal-to-noise ratio, the absolute values of Q RX channels are accumulated. Subsequently, coarse target detection is performed by implementing a clutter cancelation algorithm [2] and generating $K\times$ RD maps by conducting 2D fast Fourier transform (FFT), obtaining sizes $N_R^{(\mathrm{r})}$ reduced from N_R and $N_D^{(\mathrm{r})}$ reduced from N_D for the range and Doppler estimations, respectively. If the target is not detected, the algorithm does not proceed to Step 2, but instead returns to the beginning of Step 1. Conversely, if an approximate region pertaining to the target is detected, U beam indices $(=\hat{k}_1,\hat{k}_2,\dots\hat{k}_U)$ are estimated for the region where the target is estimated to exist, after which Step 2 commences. In Step 2, 2D FFT is performed on beat signals of size $N_R\times N_D$, meaning that their full sizes were not reduced to estimate the range and Doppler measurements corresponding to the estimated U beam indices. This process leads to a significant reduction in complexity, since 2D FFT is performed only on the beams where the target is determined to exist, as opposed to performing 2D FFT for all beams.

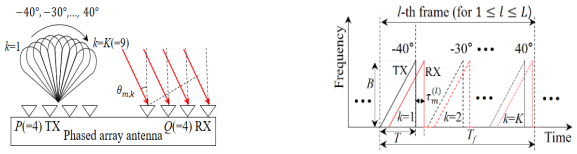

(a) (b)

Fig. 1. Structure of the TX and RX parts: (a) structure of TX and RX, and (b) beam steering TX and RX signals.

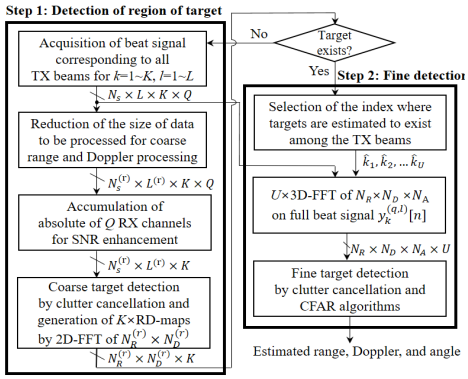

Fig. 2. Structure of the proposed algorithm.

IV. Experimental Results

Experiments were conducted to confirm the effectiveness of the proposed algorithm. Fig. 3 presents photos of the proposed radar system and the experimental setup. A 24-GHz FMCW radar system comprising a front-end module (FEM) and a back-end module (BEM) was employed. Notably, the FEM used in this study, consisting of 4 TX and 4 RX antennas, had been developed in a previous work [6], while the BEM carried out data logging in real time.

The parameters considered for the experiment are as follows: the bandwidth was 250 MHz, the chirp duration T was set to 100 μs, the pulse repetition interval was 1 ms, the number of frames L was 64, the TX power was set to 10 mW, the sampling rate was 5 MHz, the number of samples N_s was 500, and the number of TX beams K was 9. Furthermore, the size of the FFT for generating fine RD maps was set to 512 and 64, and it was reduced to 128 and 32 for generating coarse RD maps. The target with a Doppler generator was placed at a distance of 3 m at an angle of 0°. Meanwhile, the two clutters were corner reflectors with a high radar cross-section (RCS) of 10.13 dBsm stationed at distance of 2 m and at angles of −30° and 20°, respectively.

Fig. 4 shows the RD map obtained based on the TX beam index k for coarse target detection, i.e., Step 1. Due to the clutter cancelation algorithm, the two clutters at the −30° and 20° angles of the TX beam, i.e., at $k=2$ and $k=7$, are not detected despite a high RCS. However, the target is detected at a range of 3 m and a velocity of 0 m/s at $k=5$ and $k=6$.

Fig. 5 shows the RD and range-angle (RA) maps obtained in Step 2, which involved fine detection at $k=5$ and $k=6$. Compared to the

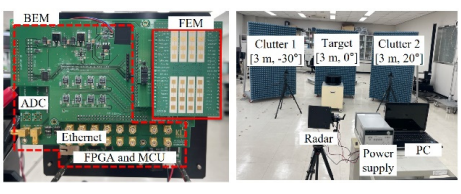

(a) (b)

Fig. 3. Experimental setup: (a) radar system and (b) photography of scenario.

results in Fig. 4(e) and 4(f), the resolution of the RD map in Fig. 5 is higher. Furthermore, the angles estimated using DBF were found to be 0° and 10° at $k = 5$ and $k = 6$, respectively. Finally, the target angle was estimated by subtracting the angle of the TX beam from the angle estimated by DBF. The proposed algorithm accurately estimated the target angle as 0° at $k = 5$ and $k = 6$. This further suggests that the proposed algorithm correctly estimated the range, velocity, and angle despite the reduction of unnecessary complexity.

Fig. 6 presents a comparison of the required memory sizes based on the number of occupied TX beams involved in the conventional [6] and proposed algorithms, with several N_Rs considered for $N_D = 64$ and $N_D = 128$. In the case of the conventional algorithm, since all beams were occupied, a constant value was observed, regardless of the x-axis. In contrast, in the proposed algorithm, the required memory size increased depending on the number of occupied beams. Overall, it is evident that the complexity is significantly reduced in the proposed algorithm, since the number of occupied TX beams is not large.

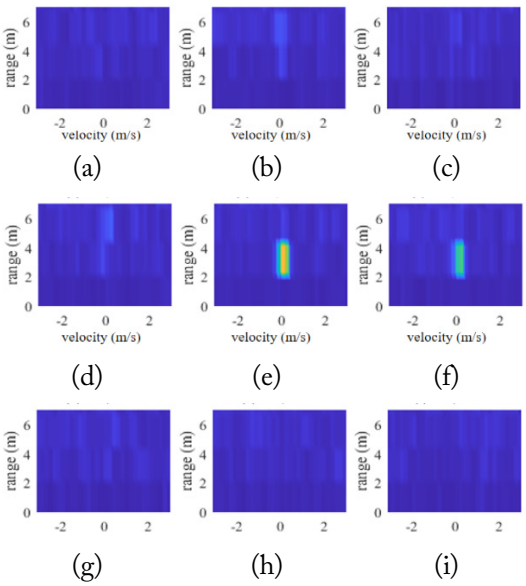

Fig. 4. Range-Doppler map based on TX beam index k: (a) $k = 1$, −40°; (b) $k = 2$, −30°; (c) $k = 3$, −20°; (d) $k = 4$, −10°; (e) $k = 5$, 0°; (f) $k = 6$, 10°; (g) $k = 7$, 20°; (h) $k = 8$, 30°; and (i) $k = 9$, 40°.

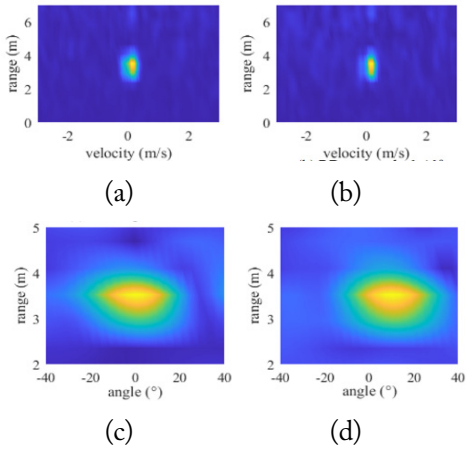

Fig. 5. Range-Doppler map for Step 2 at (a) $k = 5$, 0°; (b) $k = 6$, 10°. Range-angle map for Step 2 at (a) $k = 5$, 0°; (b) $k = 6$, 10°.

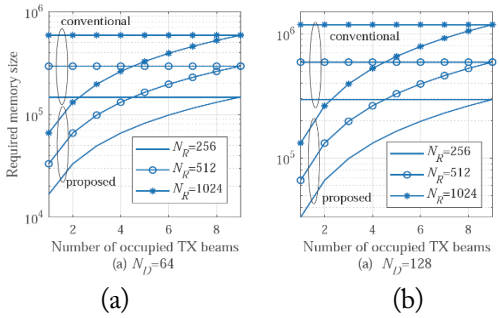

(a) (b)

Fig. 6. Comparison of required memory sizes based on the number of occupied TX beams: (a) $N_D = 64$ and (b) $N_D = 128$.

V. Conclusion

In this study, we propose a two-step adaptive target detection scheme using low-complexity beam-steering FMCW radar sensors. To reduce unnecessary computational complexity, the proposed algorithm first detected coarse information related to the target using only a portion of the data, after which high performance detection was conducted using all the data for only the beams estimated to contain the target. This procedure is expected to reduce system costs, processing time, and energy consumption.

This work was supported in part by the Institute for Information and Communications Technology Planning and Evaluation (IITP) grant funded by the Korean government (MSIT) (No. 2019-0-00138, Development of Intelligent Radar Platform Technology for Smart Environments.

References

[1] E. H. Kim and K. H. Kim, "Random phase code for automotive MIMO radars using combined frequency shift keying-linear FMCW waveform," *IET Radar, Sonar & Navigation*, vol. 12, no. 10, pp. 1090-1095, 2018. https://doi.org/10.1049/iet-rsn.2018.5075

[2] E. Hyun, Y. S. Jin, and J. H. Lee, "A pedestrian detection scheme using a coherent phase difference method based on 2D range-Doppler FMCW radar," *Sensors*, vol. 16, no. 1, article no. 124, 2016. https://doi.org/10.3390/s16010124

[3] B. S. Kim, Y. Jin, J. Bae, and E. Hyun, "Efficient clutter cancellation algorithm based on a suppressed clutter map for FMCW radar systems," *Journal of Electromagnetic Engineering and Science*, vol. 23, no. 5, pp. 449-451, 2023. https://doi.org/10.26866/jees.2023.5.l.16

[4] J. S. Park, J. P. Kim, and D. Y. Yang, "Implementation of wide angle FoV radar module for ADAS systems," *Journal of Electromagnetic Engineering and Science*, vol. 24, no. 5, pp. 477-484, 2024. https://doi.org/10.26866/jees.2024.5.r.249

[5] J. H. Yoon, Y. Park, J. E. Roh, and S. C. Park, "Multiple step interlaced beam scan to minimize the deviation of radar detection performance," *Journal of Electromagnetic Engineering and Science*, vol. 20, no. 2, pp. 125-130, 2020. https://doi.org/10.26866/jees.2020.20.2.125

[6] G. H. Ko, J. Y. Park, K. I. Oh, G. S. Kim, E. Hyun, J. R. Yang, J. G. Kim, and D. Baek, "24-GHz 4TX–4RX phased array transceiver with automatic beam steering mode for FMCW radar applications," *IEEE Transactions on Microwave Theory and Techniques*, vol. 72, no. 5, pp. 3065-3075, 2024. https://doi.org/10.1109/TMTT.2023.3320741